DOI: 10.1002/ejic.200900202

Theoretical Study of the RNA Hydrolysis Mechanism of the Dinuclear Zinc Enzyme RNase Z

Rong-Zhen Liao,[a,b] Fahmi Himo,*[b] Jian-Guo Yu,*[a] and Ruo-Zhuang Liu[a]

Keywords: Enzyme catalysis / Metalloenzymes / Dinuclear zinc enzymes / Density functional calculations / Hydrolysis / Reaction mechanisms / Zinc

RNase Z is a dinuclear zinc enzyme that catalyzes the removal of the tRNA 3′-end trailer. Density functional theory is used to investigate the phosphodiester hydrolysis mechanism of this enzyme with a model of the active site constructed on the basis of the crystal structure. The calculations imply that the reaction proceeds through two steps. The first step is a nucleophilic attack by a bridging hydroxide coupled with protonation of the leaving group by a Glu-His diad. Subsequently, a water molecule activated by the same Glu-His diad makes a reverse attack, regenerating the bridging hydroxide. The second step is calculated to be the rate-limiting step with a barrier of 18 kcal/mol, in good agreement with experimental kinetic studies. Both zinc ions participate in substrate binding and orientation, facilitating nucleophilic attack. In addition, they act as electrophilic catalysts to stabilize the pentacoordinate trigonal-bipyramidal transition states.

Introduction

RNase Z is a dinuclear zinc-dependent endoribonuclease responsible for the processing of the 3′ extremities of transfer RNA (Scheme 1) in a variety of organisms, including bacteria, archaea, and eukarya.[1] After this hydrolytic reaction, the tRNA 3′-end can be further modified by nucleotidyl transferase and aminoacyl synthetase.[2]

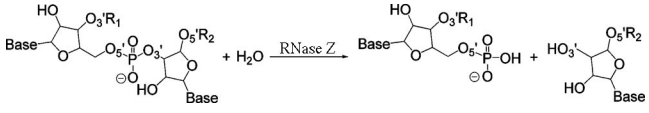

Scheme 1.

Comparisons of the amino acid sequence have demonstrated that RNase Z is a member of the metallo-β-lactamase superfamily, which catalyze primarily hydrolytic reactions of a wide range of substrates.[3] The hydrolytic water molecule is activated for nucleophilic attack by coordination to a mononuclear or dinuclear metal center. These enzymes fold into a four-layer αβ/βα sandwich fold and possess the characteristic "histidine motif" (HxHxDH) for metal coordination.[4] However, RNase Z has a unique exosite inserted in the metallo-β-lactamase domain, which is essential for tRNA recognition but not responsible for the catalytic activity.[5]

The X-ray structures of RNase Z from *Bacillus subtilis*, *T. maritime*, and *E. coli* have been solved and reveal a dinuclear zinc cluster at the active site.[5c,6] The two subunits of free *Bacillus subtilis* RNase Z dimer display different conformational states.[6a] The A-subunit possesses a functional active site to which a phosphate ion is bound, while the B-subunit, lacking zinc ions, is proposed to be structurally adapted to substrate recognition and binding. The dinuclear zinc center is bridged by an aspartate (Asp211) and an oxygen species (see Figure 1). Zn_α is liganded by three histidine residues (His63, His65, and His140), while Zn_β is liganded by two histidine and one aspartate residues (His68, His269 and Asp67). Mutational studies of these first-shell ligands show that all of them are functionally important.[7] A Glu231-His247 diad is located close to the dinuclear core and forms a hydrogen bond to one of the phosphate oxygen atoms.

On the basis of the crystallographic studies and mechanistic data concerning the related metallo-β-lactamase superfamily, the following mechanism for precursor tRNA cleavage has been proposed.[6a] Asp67 acts as a general base to remove the proton from the bridging water molecule to generate a hydroxide, which performs an in-line nucleophilic attack on the phosphorus moiety. Then, the 3′-oxygen of the discriminator base takes up a proton from the nearby water molecule. However, the substitution of Glu630 or His646 with alanine in *D. melanogaster* RNase Z (corre-

[a] College of Chemistry, Beijing Normal University, Beijing, 100875, P. R. China
E-mail: jianguo_yu@bnu.edu.cn
[b] Department of Organic Chemistry, Arrhenius Laboratory, Stockholm University, 10691 Stockholm, Sweden
E-mail: himo@organ.su.se

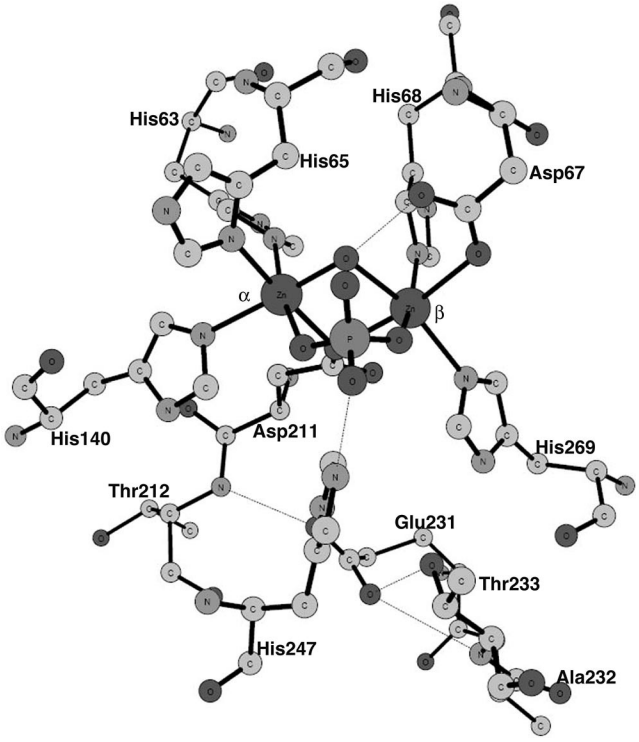

Figure 1. X-ray structure of the active site of RNase Z from *Bacillus subtilis* complexed with phosphate (coordinates taken from PDB entry 1Y44).

sponding to Glu231 and His247 in *B. subtilis* RNase Z, see Figure 1) causes a dramatic decrease in k_{cat}, indicating that the Glu-His diad might act as a general acid involved in the protonation of the leaving group.[7c] This proposal has also been put forward for another dinuclear zinc-dependent phosphodiesterase, namely CPSF-73 (73-kDa subunit of cleavage and polyadenylation specificity factor) involved in pre-mRNA 3′-end processing, with identical disposition and coordination of the dinuclear zinc core in the active site.[8] The structure of CPSF-73 reveals that a sulfate is directly coordinated to the two zinc ions, and a Glu204-His396 diad is hydrogen-bonded to one of the sulfate oxygen.

In the current study, we used density functional theory (DFT) calculations to investigate the phosphodiesterase activity of RNase Z. With the aim to study the detailed reaction mechanism and characterize the involved transition states and intermediates, we constructed a model of the active site on the basis of the crystal structure of the native RNase Z (Protein Data Bank entry 1Y44),[6a] and employed the hybrid density functional method B3LYP[9] to present a potential energy surface for the reactions. This approach has previously been applied very successfully to a number of enzymes,[10] including five recent studies on related dinuclear zinc enzymes.[11] The results presented here can be extended to the reaction mechanisms of CPSF-73[8] and RNase J,[12] which possess identical catalytic sites as RNase Z.

Computational Details

Calculations

The calculations presented herein were carried out using the DFT functional B3LYP as implemented in the Gaussian03 program package.[13] For geometry optimization, the 6-31G(*d,p*) basis set was used for the C, N, O, H elements, the 6-311+G(*d*) for P, and the LANL2DZ[14] pseudopotential for Zn. Based on these optimized geometries, single-point calculations at the B3LYP/6-311+G(*2d,2p*) level were performed to obtain more accurate energies. Single point calculations at the MPWB1K/6-311+G(*2d,2p*) level[15] based on the same geometries were carried out to evaluate the accuracy of barriers and reaction enthalpies. MPWB1K was found to give very close relative energies compared to B3LYP (less than 1 kcal/mol difference).

The dielectric effects from the protein surroundings that were not explicitly included in the model were calculated at the same theory level as the geometry optimizations using the conductor-like polarizable continuum model (CPCM) method, where a solvent cavity is formed as a surface of constant charge density of the solvated molecule.[16] The dielectric constant was set equal to four, which is the standard value used in modeling protein surroundings. Zero-point energy (ZPE) effects were computed by performing frequency calculations at the same theory level as the optimizations. Some truncation atoms were kept fixed to their crystallographically observed positions. This procedure gives rise to several small imaginary frequencies, typically on the order of 10*i*–30*i* cm^{-1}. These do not contribute significantly to the ZPE and can thus be ignored. The energies reported herein are corrected for both solvation and ZPE. The adequacy of some of the technical aspects of this modeling approach with respect to dinuclear zinc enzymes was tested in a recent study on the reaction mechanism of phosphotriesterase.[17]

Active-Site Model

A quantum chemical cluster model of the RNase Z active site was prepared on the basis of the crystal structure of the enzyme complexed with phosphate (PDB entry 1Y44).[6a] The model consists of the two zinc ions along with their first-shell ligands, His63, His65, Asp67, His68, His140, Asp211, His369 and the bridging hydroxide. Glu231 and His247, which are possibly involved in protonating the leaving group, were also included in the model. The histidines were modeled by methylimidazoles, while the glutamate and aspartate residues were modeled by acetates. Additionally, parts of the Asp211-Thr212 and Ala232-Thr233 units, forming hydrogen bonds with Glu231, were included. Hydrogen atoms were added manually. The bridging ligand is assumed to be a hydroxide. This is a reasonable assumption, since the pK_a of a water molecule will be very low when coordinated to two zinc ions, especially when the dizinc center has only two negatively charged ligands. The

same assumption has also been made for the other dizinc enzymes studied previously.[11] To keep the optimized structures close to the experimental one, the truncation atoms were fixed at their corresponding X-ray positions during the geometry optimizations. The fixed atoms are marked with asterisks in the figures below. A simple model substrate, methyl 2-tetrahydrofuranyl phosphate, was used to explore the phosphodiesterase activity of this enzyme (see Figure 2). The resulting model is composed of 139 atoms and has a total charge of 0.

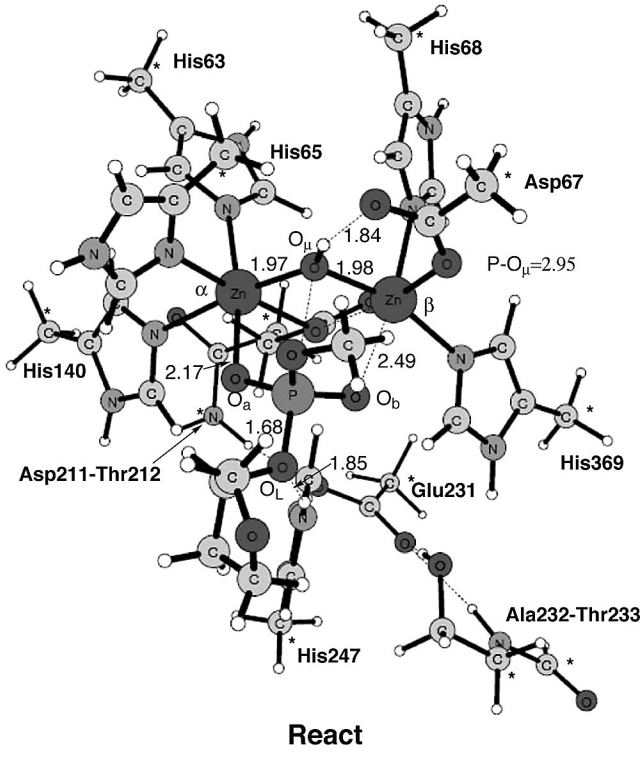

Figure 2. Optimized structure of the RNase Z active site model with a methyl 2-tetrahydrofuranyl phosphate bound. Atoms marked with asterisks were fixed at their X-ray structure positions. Distances are given in Å.

Results and Discussion

The optimized structure of the RNase Z active site with the methyl 2-tetrahydrofuranyl phosphate substrate bound, corresponding to the Michaelis complex (here termed **React**), is shown in Figure 2. The overall geometric parameters obtained from the geometry optimization reproduce the X-ray structure quite well. For example, the Zn_α–Zn_β distance is calculated to be 3.37 Å, which is in very good agreement with the crystallographic distance of 3.30 Å.[6a] Also, the hydrogen bonds between the bridging hydroxide ($O_\mu H^-$) and Asp67, and between the leaving oxygen (O_L) and His247 are well-reproduced. The geometry optimization was initially started with neutral His247 and Glu231 residues. However, during the optimization, a proton was transferred automatically from Glu231 to His247 creating a Glu^-–$HisH^+$ ion pair. The resulting Glu231 anion is stabilized through hydrogen bonds to the Ala232-Thr233 and Asp211-Thr212 moieties. The substrate is coordinated to the two zinc ions with two of its phosphate oxygen atoms, where O_a binds to Zn_α (Zn_α–O_a: 2.17 Å) stronger than O_b to Zn_β (Zn_β–O_b: 2.49 Å). This is because the Zn_α ion is more positively charged, due to its ligands. These interactions help orient the substrate so that there is a nearly straight line between O_μ–P–O_L, with an angle of 178.1°. The O_μ–P distance is 2.95 Å and the substrate is thus ready for the nucleophilic attack.

The optimized transition state (TS**1**) and the resulting intermediate (Inter**1**) are shown in Figure 3. We find that the nucleophilic attack occurs directly from the bridging position, similar to other previously studied dinuclear zinc enzymes, phosphotriesterase (PTE),[11a] aminopeptidase from *Aeromonas proteolytica* (AAP),[11b] dihydroorotase (DHO),[11c] *N*-acyl-L-homoserine lactone hydrolase (AHL lactonase),[11d] glyoxalase II (GlxII).[11e] The nature of TS**1** was confirmed to have an imaginary frequency of 756*i*cm^{-1}, which corresponds to the O_μ–P bond formation and P–O_L bond breakage, coupled with proton transfer from His247 to O_L. The barrier is calculated to be 13.6 kcal/mol (14.3 kcal/mol without the solvation correction) and Inter**1** is found to be 6.6 kcal/mol lower than **React** (10.4 kcal/mol without the solvation correction). At TS**1**, both the critical O_μ–P and P–O_L distances are 1.98 Å. In addition, the transferring proton is approximately in the middle of N_ε (His247) and O_L, where the key distances of the proton to Nε and O_L are 1.28 and 1.22 Å, respectively. The Zn_α–O_a and Zn_β–O_b bonds become somewhat shorter (2.10 Å and 2.24 Å, respectively), which indicates that the zinc ions provide electrostatic stabilization to the transition state, thereby lowering the barrier.

Downhill from TS**1**, a proton transfer from the bridging hydroxide to Asp67 occurs simultaneously with the dissociation of the leaving group. The leaving alcohol can easily be released to the solution as it is only hydrogen-bonded to His247. However, the direct release of the phosphomonoester from Inter**1** will require much more energy since it is strongly bound to the dinuclear center. An alternative pathway is that a water molecule makes the reverse attack on the phosphorus center regenerating the bridging hydroxide, which then can start a new catalytic cycle. Accordingly, we manually replaced the alcohol in Inter**1** by a water molecule and reoptimized the geometry (called Inter**2**, Figure 3). The energy difference between Inter**1** and Inter**2** can be roughly estimated by the following equation:

Inter**1** (ε = 4) + H_2O (ε = 80) → Inter**2** (ε = 4) + Alcohol (ε = 80)

According to this equation, the step is calculated to be exothermic by 4.7 kcal/mol (10.1 kcal/mol without the solvation correction). However, this is to be considered as a crude approximation, since the solvation energies of the water molecule and the alcohol are not expected to be very accurate using the implicit solvent model.

From Inter**2**, we have optimized the transition state for the water attack at the phosphorus center (TS**2**, Figure 3). The barrier is calculated to be 18.1 kcal/mol (22.8 kcal/mol

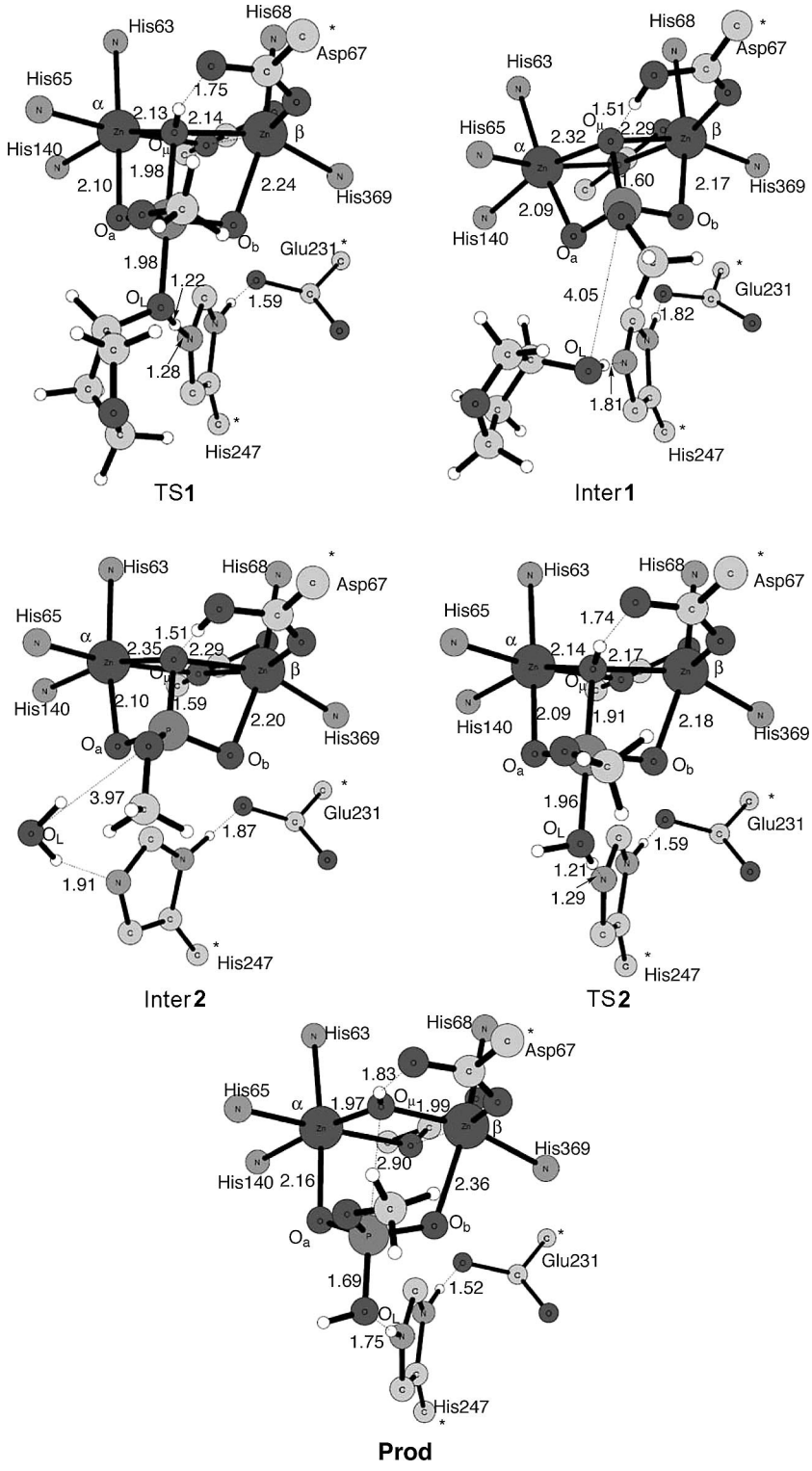

Figure 3. Optimized geometries for the transition states, intermediates and product along the reaction pathway. For clarity, the zinc-coordinated histidine rings, Ala232-Thr233, part of Asp211-Thr212, and unimportant hydrogen atoms are omitted.

without the solvation correction) relative to Inter**2**. In TS**2**, His247, facilitated by the negative charge of Glu231, abstracts a proton from the water molecule. The geometry of TS**2** is found to be very similar to that of TS**1**. The distance between the phosphorus and the water oxygen is 1.96 Å, while the water proton is 1.21 Å from the water oxygen and 1.29 Å from the N_ε atom of His247. This water attack results in the formation of the product (**Prod**, Figure 3) with the regeneration of the bridging hydroxide. The second step is found to be endothermic by 7.9 kcal/mol [**Prod** is 7.9 kcal/mol (10.7 kcal/mol without the solvation correction) higher than Inter**2**].

The obtained potential energy curve for the phosphodiester hydrolysis reaction is shown in Figure 4. From this, it can be seen that the second half-reaction determines the reaction rate, with a barrier of 18.1 kcal/mol. Experimental rate constants are found to be in the range of 0.003–0.09 s^{-1},[7,18] which can be converted to barriers in the range of 19–21 kcal/mol using classical transition state theory. Our calculations are thus in good agreement with the experimental kinetics results.

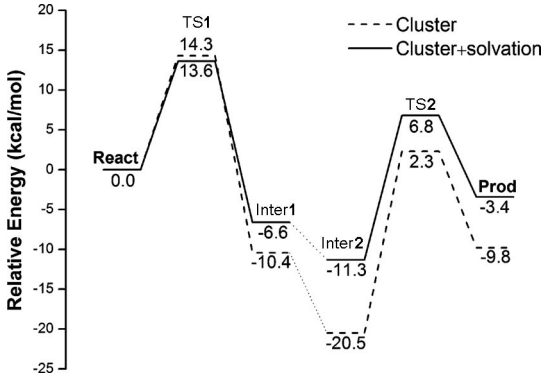

Figure 4. Calculated potential energy curve for the hydrolysis of methyl 2-tetrahydrofuranyl phosphate by RNase Z.

Conclusions

In this work, we have used density functional theory calculations to investigate the RNA hydrolysis mechanism by RNase Z. Our calculations established the following mechanistic features (Scheme 2): (1) The phosphate group of the substrate binds to the active site mainly through direct bidentate coordination to the dinuclear zinc center and hydrogen bonding to His247. (2) The bridging hydroxide, coordinated to the two zinc ions, performs the nucleophilic attack directly from bridging position. This seems to be a common feature for dinuclear zinc hydrolases and has been demonstrated for several other related enzymes.[11] (3) The nucleophilic attack on the phosphorus center results in the concerted departure of the leaving group, which accepts a proton from His247. In the subsequent step, a water molecule, activated by His247, makes the reverse attack resulting in the regeneration of the bridging hydroxide. (4) The second step is rate-limiting and the energetic barrier is calculated to be 18.1 kcal/mol, in good agreement with experimental kinetic studies. (5) Asp67 acts first as a general base to accept a proton from the bridging hydroxide in the first half-reaction and to return it in the second half-reaction. Both zinc ions provide catalytic power by the electrostatic stabilization of the pentacoordinate transition states.

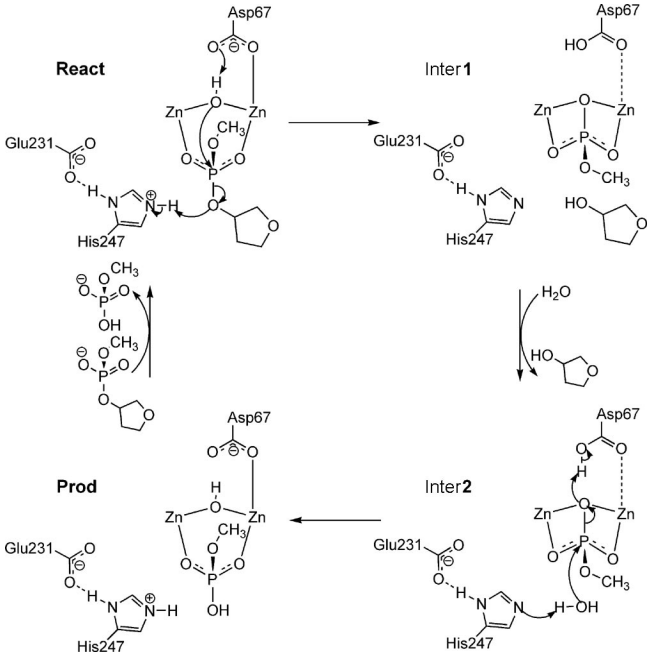

Scheme 2. Suggested RNA hydrolysis mechanism by RNase Z.

Acknowledgments

F. H. gratefully acknowledges financial support from The Swedish National Research Council (VR), The Carl Trygger Foundation, and The Magn Bergvall Foundation. This work was also supported by grants from the National Natural Science Foundation of China (Grants 20733002 and 20873008) and Major State Basic Research Development Programs (Grants 2004CB719903 and 2002CB613406).

[1] a) H. Takaku, A. Minagawa, M. Takagi, M. Nashimoto, *Nucleic Acids Res.* **2004**, *32*, 4429–4438; b) A. Vogel, O. Schilling, B. Späth, A. Marchfelder, *Biol. Chem.* **2005**, *386*, 1253–1264; c) Y. Redko, I. Li de la Sierra-Gallay, C. Condon, *Nat. Rev. Microbiol.* **2007**, *10*, 271–278; d) B. Späth, G. Canino, A. Marchfelder, *Cell. Mol. Life Sci.* **2007**, *64*, 2404–2412.

[2] a) M. P. Deutscher, *Enzymes* **1982**, *15*, 183–215; b) M. Ibba, D. Söll, *Annu. Rev. Biochem.* **2000**, *69*, 617–650.

[3] S. V. Tavtigian, J. Simard, D. H. F. Teng, V. Abtin, M. Baumgard, A. Beck, N. J. Camp, A. R. Carillo, Y. Chen, P. Dayananth, M. Desrochers, M. Dumont, J. M. Farnham, D. Frank, C. Frye, S. Ghaffari, J. S. Gupte, R. Hu, D. Iliev, T. Janecki, E. N. Kort, K. E. Laity, A. Leavitt, G. Leblanc, J. McArthur-Morrison, A. Pederson, B. Penn, K. T. Peterson, J. E. Reid, S. Richards, M. Schroeder, R. Smith, S. C. Snyder, B. Swedlund, J. Swensen, A. Thomas, M. Tranchant, A.-M. Woodland, F. Labrie, M. H. Skolnick, S. Neuhausen, J. Rommens, L. A. Cannon-Albright, *Nat. Genet.* **2001**, *27*, 172–180.

[4] L. Aravind, *In Silico Biol.* **1999**, *1*, 69–91.

[5] a) B. Späth, S. Kirchner, A. Vogel, S. Schubert, P. Meinlschmidt, S. Aymanns, J. Nezzar, A. Marchfelder, *J. Biol. Chem.* **2005**, *280*, 35440–35447; b) O. Schilling, A. Vogel, B. Kostelecky, H. Natal da Luz, D. Spemann, B. Späth, A. Marchfelder, W. Tröger, W. Meyer-Klaucke, *Biochem. J.* **2005**, *385*, 145–153; c) I. Li de la Sierra-Gallay, N. Mathy, O. Pellegrini, C. Condon, *Nat. Struct. Mol. Biol.* **2006**, *13*, 376–377; d) A. Minagawa, R. Ishii, H. Takaku, S. Yokoyama, M. Nashimoto, *J. Mol. Biol.* **2008**, *381*, 289–299.

[6] a) I. Li de la Sierra-Gallay, O. Pellegrini, C. Condon, *Nature* **2005**, *433*, 657–661; b) R. Ishii, A. Minagawa, H. Takaku, M. Takagi, M. Nashimoto, S. Yokoyama, *J. Biol. Chem.* **2005**, *280*, 14138–14144; c) B. Kostelecky, E. Pohl, A. Vogel, O. Schilling, W. Meyer-Klaucke, *J. Bacteriol.* **2006**, *188*, 1607–1614; d) R. Ishii, A. Minagawa, H. Takaku, M. Takagi, M. Nashimoto, S. Yokoyama, *Acta Crystallogr., Sect. F* **2007**, *63*, 637–641.

[7] a) N. Zareen, H. Yan, A. Hopkinson, L. Levinger, *J. Mol. Biol.* **2005**, *350*, 189–199; b) A. Minagawa, H. Takaku, R. Ishii, M. Takagi, S. Yokoyama, M. Nashimoto, *Nucleic Acids Res.* **2006**, *34*, 3811–3818; c) S. Karkashon, A. Hopkinson, L. Levinger, *Biochemistry* **2007**, *46*, 9380–9387; d) R. A. Elbarbary, H. Takaku, M. Nashimoto, *Biochim. Biophys. Acta* **2008**, *1784*, 2079–2085.

[8] C. R. Mandel, S. Kaneko, H. Zhang, D. Gebauer, V. Vethantham, J. L. Manley, L. Tong, *Nature* **2006**, *444*, 953–956.

[9] a) A. D. Becke, *J. Chem. Phys.* **1993**, *98*, 5648–5652; b) C. Lee, W. Yang, R. G. Parr, *Phys. Rev. B* **1988**, *37*, 785–789.

[10] Reviews a) F. Himo, P. E. M. Siegbahn, *Chem. Rev.* **2003**, *103*, 2421–2456; b) L. Noodleman, T. Lovell, W.-G. Han, J. Li, F. Himo, *Chem. Rev.* **2004**, *104*, 459–508; c) P. E. M. Siegbahn, T. Borowski, *Acc. Chem. Res.* **2006**, *39*, 729–738; d) F. Himo, *Theor. Chem. Acc.* **2006**, *116*, 232–240; e) M. J. Ramos, P. A. Fernandes, *Acc. Chem. Res.* **2008**, *41*, 689–698.

[11] a) S.-L. Chen, W.-H. Fang, F. Himo, *J. Phys. Chem. B* **2007**, *111*, 1253–1255; b) S.-L. Chen, T. Marino, W.-H. Fang, N. Russo, F. Himo, *J. Phys. Chem. B* **2008**, *112*, 2494–2500; c) R.-Z. Liao, J.-G. Yu, F. M. Raushel, F. Himo, *Chem. Eur. J.* **2008**, *14*, 4287–4292; d) R.-Z. Liao, J.-G. Yu, F. Himo, *Inorg. Chem.* **2009**, *48*, 1442–1448; e) S.-L. Chen, W.-H. Fang, F. Himo, *J. Inorg. Biochem.* **2009**, *103*, 274–281.

[12] I. Li de la Sierra-Gallay, L. Zig, A. Jamalli, H. Putzer, *Nat. Struct. Mol. Biol.* **2008**, *15*, 206–212.

[13] Gaussian 03 (revision D.01), M. J. Frisch, G. W. Trucks, H. B. Schlegel, G. E. Scuseria, M. A. Robb, J. R. Cheeseman, J. A. Montgomery Jr., T. Vreven, K. N. Kudin, J. C. Burant, J. M. Millam, S. S. Iyengar, J. Tomasi, V. Barone, B. Mennucci, M. Cossi, G. Scalmani, N. Rega, G. A. Petersson, H. Nakatsuji, M. Hada, M. Ehara, K. Toyota, R. Fukuda, J. Hasegawa, M. Ishida, T. Nakajima, Y. Honda, O. Kitao, H. Nakai, M. Klene, X. Li, J. E. Knox, H. P. Hratchian, J. B. Cross, C. Adamo, J. Jaramillo, R. Gomperts, R. E. Stratmann, O. Yazyev, A. J. Austin, R. Cammi, C. Pomelli, J. W. Ochterski, P. Y. Ayala, K. Morokuma, G. A. Voth, P. Salvador, J. J. Dannenberg, V. G. Zakrzewski, S. Dapprich, A. D. Daniels, M. C. Strain, O. Farkas, D. K. Malick, A. D. Rabuck, K. Raghavachari, J. B. Foresman, J. V. Ortiz, Q. Cui, A. G. Baboul, S. Clifford, J. Cioslowski, B. B. Stefanov, G. Liu, A. Liashenko, P. Piskorz, I. Komaromi, R. L. Martin, D. J. Fox, T. Keith, M. A. Al-Laham, C. Y. Peng, A. Nanayakkara, M. Challacombe, P. M. W. Gill, B. Johnson, W. Chen, M. W. Wong, C. Gonzalez, J. A. Pople, *Gaussian*, Inc., Pittsburgh, PA, **2004**.

[14] P. J. Hay, W. R. Wadt, *J. Chem. Phys.* **1985**, *82*, 270–283.

[15] a) Y. Zhao, D. G. Truhlar, *J. Phys. Chem. A* **2004**, *108*, 6908–6918; b) Y. Zhao, D. G. Truhlar, *Acc. Chem. Res.* **2008**, *41*, 157–167.

[16] a) A. Klamt, G. Schüürmann, *J. Chem. Soc. Perkin Trans. 2* **1993**, 799–805; b) V. Barone, M. Cossi, *J. Phys. Chem. A* **1998**, *102*, 1995–2001; c) R. Cammi, B. Mennucci, J. Tomasi, *J. Phys. Chem. A* **1999**, *103*, 9100–9108; d) J. Tomasi, B. Mennucci, R. Cammi, *Chem. Rev.* **2005**, *105*, 2999–3094.

[17] S.-L. Chen, W.-H. Fang, F. Himo, *Theor. Chem. Acc.* **2008**, *120*, 515–522.

[18] a) H. S. Shibata, A. Minagawa, H. Takaku, M. Takagi, M. Nashimoto, *Biochemistry* **2006**, *45*, 5486–5492; b) B. Späth, F. Settele, O. Schilling, I. D'Angelo, A. Vogel, I. Feldmann, W. Meyer-Klaucke, A. Marchfelder, *Biochemistry* **2007**, *46*, 14742–14750.

Received: March 2, 2009
Published Online: June 5, 2009

